Supersonic and Transonic Deployment of Ribbon Parachutes at Low Altitudes

RANDALL C. MAYDEW* AND DONALD W. JOHNSON†
Sandia Laboratories, Albuquerque, N. Mex.

Results are presented for twenty-nine flight tests of a 22.2-ft (6.8-m) diameter ribbon parachute (reefed for 0.5 sec) with a nominal 2000-lb (907-kg) store. The design, fabrication, and packing of the parachute system are discussed. Low altitude drop tests were made with F-4 and A-4 aircraft at Mach numbers from 0.57 to 1.22, and rocket-boosted tests were made at Mach numbers from 1.62 to 1.70, the latter corresponding to a maximum dynamic pressure of 2720 psf (130 kN/m²). The maximum measured snatch load, reefed stage opening shock, and second stage opening shock were approximately 65 klb (289 kN), 165 klb (734 kN) and 150 klb (667 kN), respectively. The measured load data and sequence of parachute function times are relatively consistent and repeatable. There is no discernible effect of Mach number on the steady-state drag area of the reefed parachute at Mach numbers from 0.7 to 1.50.

Nomenclature

A_i, A_e = effective canopy inlet and exit areas, respectively, during inflation process
C_D = drag coefficient based on S_c
$C_D S$ = drag area, full open
D_c = constructed diameter (base of conical ribbon parachute or diameter of reefing line circle)
D_0 = nominal parachute diameter
D_E = effective reefed parachute diameter
g = acceleration
L = distance travelled during opening
L_R = length of reefing line
M = Mach number
Q = dynamic pressure
S_c = base area of parachute or area of reefing line circle
t = time from tail can ejection
Δt_f = filling time of nonreefed parachute
Δt_{1p} = time to first peak load, $t_{1p} - t_{LS}$, or approximate first stage filling time
Δt_{2f} = filling time from disreefing until full open (from optical data)
Δt_{2p} = time to second peak load, $t_{2p} - t_{DR}$
Δt_R = reefing line cutter time delay, $t_{DR} - t_{LS}$
V = vehicle velocity
V_c = volume of canopy
λ_G = geometric porosity of canopy
ρ_c = density inside canopy at full inflation
ρ_∞ = freestream static density

Subscripts

0 = conditions at tail can eject
1 = reefed conditions
2 = conditions after disreefing
DR = conditions when reefing cutter fires
LS = conditions at line stretch
p = conditions at peak loads

Received January 21, 1972; revision received March 31, 1972. This work was supported by the U.S. Atomic Energy Commission. Most of the information presented herein was presented at the Royal Aeronautical Society Symposium on Parachutes and Related Technologies, September 15–16, 1971, London, England. The flight tests were conducted by Sandia Laboratories in conjunction with the U.S. Air Force who supplied the parachutes. The efforts of C. A. Schreiber, managing of the flight test program; E. W. Hall, design and assembly of rocket system; and A. E. McIntyre, data analysis, are appreciated. The contributions of R. L. Hester, Jr., ASD(ENCDP), Wright-Patterson Air Force Base, Ohio, are particularly noted and appreciated.

Index categories: Aircraft Deceleration Systems; Post-Entry Deceleration Systems and Flight Mechanics.

* Manager, Aerodynamics Projects Department.

† Member of Technical Staff, Deceleration and Recovery Systems Division, Aerodynamics Projects Department.

Introduction

HEAVY duty ribbon parachutes[1,2] have been designed and extensively used at Sandia Laboratories for the past 17 yrs in the development of retardation systems for nuclear and other ordnance. Ribbon parachutes from 1–130 ft (0.3–39.6 m) diam, used to decelerate vehicles weighing 5–45,000 lb (2.3–20,412 kg), have been designed and tested. A reefed 20-ft (6.1-m) diam ribbon parachute, constructed of reinforced selvage ribbons of up to 4000-lb (17.8-kN) tensile strength, has been tested[3] at dynamic pressures up to 5700 psf (272 kN/m²) resulting in 178 klb (792 kN) opening shock loads on the 1100-lb (499-kg) test vehicle.

A 22.2-ft (6.8-m) diam ribbon parachute (reefed for 0.5 sec) was recently developed for decelerating a nominal 2000-lb (907-kg) store released at low-altitude, low supersonic Mach number conditions. Twenty-nine instrumented field tests of this parachute/store were made using F-4 and A-4 aircraft at release Mach numbers of 0.57 to 1.22 and rocket-boosted vehicles at test Mach numbers of 1.62 to 1.70. This paper presents the results of these tests along with information on the design, construction and packing of this parachute system.

Test Vehicles

The vehicle used for the rocket-boosted tests is 18 in. (0.46 m) in diameter, 164 in. (4.17 m) long and weighs 2140 lb (971 kg). Two aft-looking cameras for photographing the deployment and operation of the parachute are mounted between the vehicle fins. The vehicle is held to the forward end of an Honest John rocket motor by an interstage structure. The complete system, installed on a rail-type launcher, is shown in Fig. 1. The system is launched at an elevation angle of 30°. After burnout of the rocket motor (about 5 sec after launch), the test vehicle and motor separate due to the difference in the drag of the two bodies. At this time the test vehicle Mach number is 1.97, the altitude is 2100 ft (640 m) above ground level, and the dynamic pressure is 4350 psf (208 kN/m²). The vehicle then coasts to the desired test condition of, say, Mach number of 1.7; at this point its altitude is 6470 ft (1972 m) above ground level and the dynamic pressure is 2670 psf (128 kN/m²). Closure of a pressure switch (note the nose-mounted Pitot probe in Fig. 1) initiates

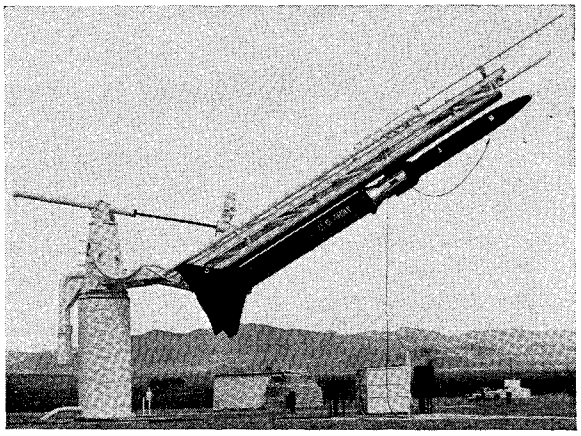

Fig. 1 Rocket-boosted test system.

explosive separation of the tail can from the test vehicle, deploying the pilot parachute.

The test vehicle used for the aircraft drops weighs 2005 lb (909 kg) and has the same design (except there are no camera mounts) as the vehicle used on the rocket-boosted tests. Closure of a timer 0.6 sec after release from the aircraft initiates explosive separation of the tail can from the test vehicle, deploying the pilot parachute.

Parachute System

The 22.2-ft (6.8-m) ribbon parachute pack is shown in Fig. 2. It is constructed of nylon materials and includes 32 gores, as shown in Fig. 3. The horizontal ribbons are continuous around the canopy. All the horizontal ribbons have reinforced selvage.[1] The calculated geometric porosity of the canopy is 23%. Pocket bands are used on the canopy to aid inflation. The suspension lines are continuous over the canopy vent and through the test vehicle lugs with the splices placed in the canopy vent area. One piece of webbing is used to form four suspension lines, thus keeping the number of joints or splices to a minimum. The suspension line length is 23.75 ft (7.24 m) of which 4 ft (1.22 m) is inside the test vehicle. A reefing system is incorporated into the canopy to control the opening load. Steel reefing rings are attached to thirty of the skirt reinforcement-suspension line joints. Reefing line cutters are bolted on the two remaining diametrically-opposed joints. A 9000-lb, 1-in. (40-kN, 2.5-cm) wide webbing, 19.25 ft (5.87 m) long, is normally used for the reefing line; the line is cut 0.5 sec after parachute line stretch.

The pilot parachute is a 3-ft (0.9-m) diam ribless guide surface parachute constructed by the method described by Solt.[4] The parachute has 8 gores with the canopy fabricated from 14 oz/yd^2 (0.47 kg/m^2) nylon material and the suspension lines constructed from 6000-lb, 1-in. (26.7-kN, 2.5-cm) wide nylon webbing.

The deployment bag (Fig. 2) is constructed of two panels which attach to a flat end to form a cylindrical bag 10.5 in. (0.27 m) in diam and 50 in. (1.27 m) long. The panels have grommets for lacing; the canopy and suspension lines are tied to loops sewn on the inside of the panels. Longitudinal

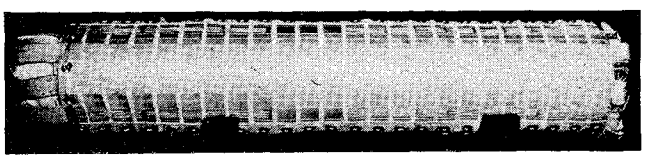

Fig. 2 Parachute pack.

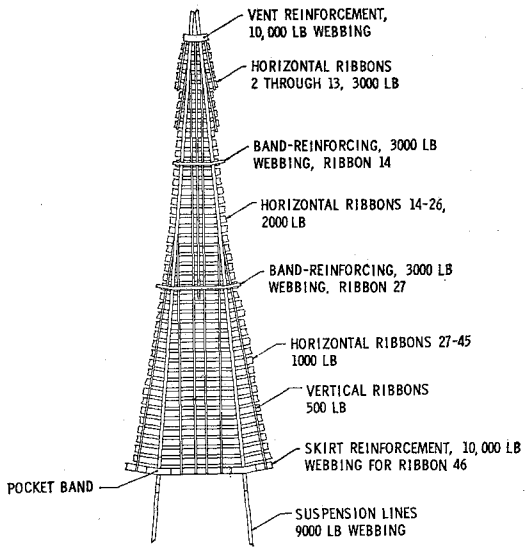

Fig. 3 Typical gore construction for 22.2 ft (6.8 m) diam 20° conical ribbon parachute.

webbings are sewn to each panel to withstand the pilot parachute load during deployment of the main parachute.

During packing, the parachute canopy and suspension lines are divided into two groups and each group is tied to the loops on a panel of the deployment bag. The canopy is tied to each panel in 4 places with 200-lb (890-N) nylon tape, and the suspension lines are tied to each panel in 25 places with 200-lb (890-N) tape. This method of packing is described by Widdows.[6] The two panels are then laced together to form a cylindrical bag. Rigged knives cut the lacing during parachute deployment, thus preventing friction burns. Volume limitations require a very dense pack. Mechanical assistance is needed in tightening the laces and a 40-klb (178-kN) hydraulic press along with clam shell forms are used to obtain the final packed shape. Sixteen manhours are required for both the initial packing and for bag tightening.

The pilot parachute is packed in a deployment bag which is attached to the end of the main deployment bag (Fig. 2). The finished pack is 10.5 in. (0.27 m) in diameter and 60 in. (1.5 m) long. The total weight is 135 lb (61.2 kg).

Test Range and Instrumentation

The tests were conducted at the Sandia Laboratories Tonopah Test Range[7] which is located in Nevada at an elevation of 5330 ft (1625 m) above sea level. The range has radar tracking, excellent optical instrumentation, and telemetry receiving capability.

An FM/FM analog telemetry system was used on both the air-drop and the rocket-boosted tests. Data acquired included accelerations, time sequences and Pitot pressure (rocket-boosted tests only). The frequency response of the test vehicle accelerometers was 800 Hz. The acceleration data were processed from magnetic tape through an analog-to-digital converter and machine plotted as shown in Fig. 4. The accuracy of the data is estimated to be within 5%.

Extensive optical instrumentation was used on the tests. Two aft-looking 16-mm cameras (200 and 1000 frames/sec) were mounted on the rocket-boosted test vehicle to photograph the deployment and opening process of the parachute. Generally, four tracking telescopes with 35- and 70-mm cameras (96 or 200 frames/sec) were operated on each test to provide documentary pictures and event-time information. At least three Contraves cinetheodolites (10 frames/sec) were operated on each test to provide angle data which are used to determine space positioning of the test vehicle. The space

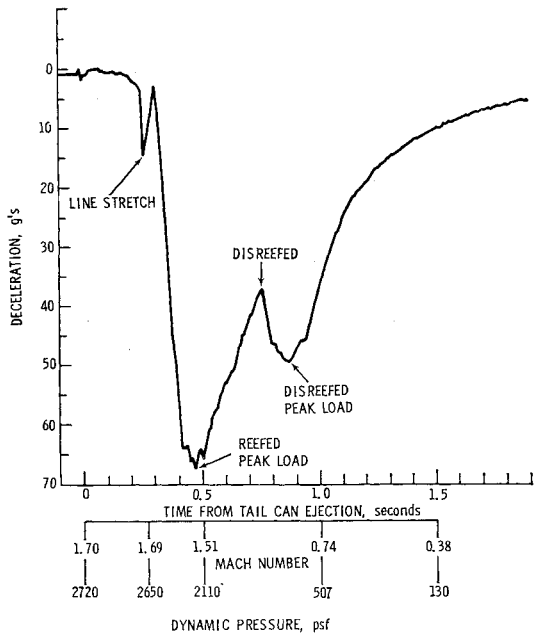

Fig. 4 Typical vehicle deceleration record.

position data are combined with the meteorologic data (taken at the time of the test) in a high-speed computer to calculate the trajectory of the test vehicle along with the velocity, dynamic pressure and Mach number vs time. The originally calculated space position data are estimated to have a relative accuracy of less than 1 ft.

The accuracy of dynamic pressure (velocity) data during periods of high velocity change (i.e., 20–70 g deceleration) determined from theodolites may be suspect. The accuracy of the dynamic pressure (velocity) data used in this paper is indirectly indicated in Fig. 5 which shows the parachute steady-state drag area vs time calculated by two different methods at intervals of 0.05 sec. The solid line represents the method in which C_DS was calculated directly from the accelerometer load data and theodolite-determined dynamic pressure. The dashed line is based on utilization of integrated accelerometer data to determine the velocity changes to the theodolite-determined initial velocity during the periods of parachute opening (high deceleration). The correct calibration of the accelerometer data is insured by forcing the velocity determined by this method to agree with the theodolite-determined velocity after the period of high deceleration. This corrected velocity was then used to calculate dynamic pressure and the C_DS (using the transient accelerometer load data) shown as the dashed line in Fig. 5. These curves indicate the dynamic pressure determined from theodolite data is sufficiently accurate.

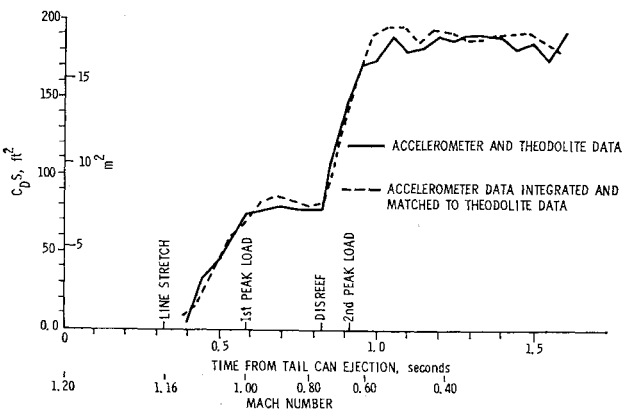

Fig. 5 Comparison of two methods of determining steady-state drag area, test A360.

Results

Aerodynamic parameters, peak loads and event times are presented in Table 1. The deceleration load (g's) tabulated was chosen from the least noisy of the three telemetering channels (usually the highest carrier frequency). These same accelerometer records were used to calculate steady-state drag areas after the first and second stage peak loads. The nominal reefing line cutter time delay is 0.5 sec. The rms value for the tests is 0.506 sec and the standard deviation is 0.020 sec. The filling time, Δt_{2f}, of the second stage (as determined from camera data) is not too consistent and is usually longer than the time, Δt_{2p}, to the second peak load. The Δt_{2f} determination requires studying the film and arbitrarily judging when the canopy was inflated, whereas the Δt_{2p} measurement is determined (see Fig. 4) from two deceleration record peaks. The canopy is usually still inflating when the second peak load occurs.

The significant parachute function times (measured from tail can ejection) are presented in Fig. 6 as a function of the dynamic pressure at line stretch. In general, the function times are consistent and very repeatable. The second stage filling time for the shorter reefing line system [$L_R = 15.5$ ft (4.7 m)] is considerably longer than for the 19.25-ft (5.87-m) reefing line system. Examination of the onboard movie film showed the smaller skirt inlet was distorting and oscillating during the reefed stage. This indicated that a marginal pressure differential existed across the canopy which would result in a longer second stage filling time.

The first stage filling time data are compared with calculated values in Fig. 7 as a function of velocity at line stretch. It should be pointed out that there is no theoretical work available (to the authors' knowledge) on the filling times of reefed ribbon parachutes under noninfinite mass conditions. Eq. (1), presented by Solt,[4] was developed for predicting the filling time for a single-stage ribbon parachute under infinite mass conditions

$$\Delta t_f = 0.65\lambda_G D_0 / V_{LS} \tag{1}$$

An effective diameter, D_E, for the reefed parachute was used for D_0 based on the following:

$$D_E = D_c[(C_DS)_1/(C_DS)_2]^{1/2} \tag{2}$$

The effective diameter was calculated for $D_c = 22.23$ ft (6.8 m), $(C_DS)_1 = 78$ ft² (7.25 m²) and $(C_DS) = 189$ ft²

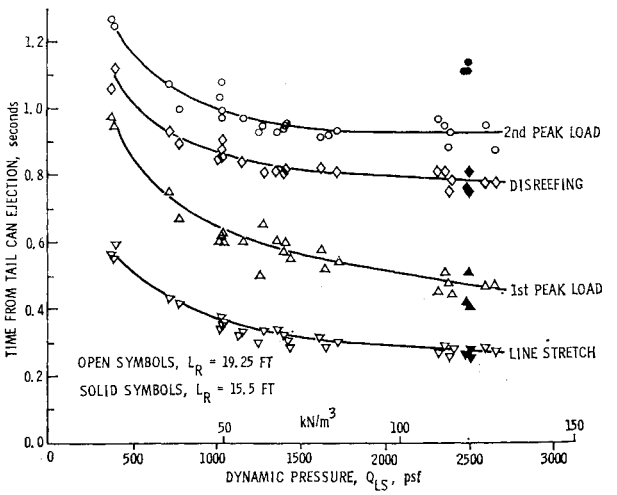

Fig. 6 Significant function times during parachute deployment and inflation.

Table 1 Test conditions, sequence times, and peak loads

Test No.	Tail Can Ejection		Line Stretch					First Peak Load						Disreefing						Second Peak Load						
	M_o	Q_o	t_{LS}	M_{LS}	V_{LS}	Q_{LS}	g_{LS}	Δt_{1p}	t_{1p}	M_{1p}	V_{1p}	Q_{1p}	g_{1p}	Δt_R[b]	t_{DR}	M_{DR}	V_{DR}	Q_{DR}	g_{DR}	Δt_{2p}	Δt_{2f}	t_{2p}	M_{2p}	V_{2p}	Q_{2p}	g_{2p}
A359X[a]	.57	389	.57	.55	616	377	5.7	.41	.98	.49	547	297	11.8	.49	1.06	.47	520	269	9.6	.21	.22	1.31	.39	437	175	14.6
A361X	.58	398	.55	.57	628	392	6.1	-	-	-	-	-	-	-	-	-	-	-	-	-	-	-	-	-	-	-
A368Y	.58	405	.59	.57	642	397	5.3	.36	.95	.53	588	333	14.7	.52	1.11	.47	525	267	9.5	.14	-	1.25	.41	461	205	17.7
A363Y	.78	737	.43	.77	848	717	8.6	.32	.75	.68	746	556	23.6	.50	.93	.57	634	400	15.0	.14	.09	1.07	.49	536	287	27.4
A364Y	.81	797	.41	.80	899	784	9.6	.26	.67	.72	804	627	30.0	.49	.90	.58	652	413	16.0	.10	.19	1.00	.51	577	322	32.2
A365Y	.92	1025	.38	.92	1020	1026	11.0	.25	.63	.80	886	776	35.0	.50	.88	.62	683	460	18.8	.09	.36	.97	.55	609	367	34.7
A362Y	.94	1051	.36	.93	1025	1040	12.6	.24	.60	.81	893	789	36.0	.49	.85	.62	690	472	17.4	.13	.12	.98	.53	586	342	34.0
A351X	.94	1064	.35	.92	1008	1026	13.7	.27	.62	.81	878	779	31.6	.55	.90	.61	668	452	16.6	.18	.31	1.08	.50	542	298	26.3
A352X	.94	1071	.34	.92	999	1021	13.5	.26	.60	.80	872	779	34.5	.51	.85	.64	690	489	19.5	.18	.36	1.03	.52	563	326	28.8
A353X	1.00	1204	.33	.98	1078	1161	18.5	.27	.60	.86	940	884	35.0	.51	.84	.67	735	542	19.9	.13	.21	.97	.57	627	395	31.8
A354X	1.00	1210	.32	.97	1069	1138	16.4	-	-	-	-	-	-	-	-	-	-	-	-	-	-	-	-	-	-	-
A367Y	1.03	1287	.31	1.01	1127	1244	14.1	.19	.50	.91	1012	1004	42.0	.50	.81	.66	728	520	20.0	.12	-	.93	.55	615	371	35.3
A357X	1.06	1351	.34	1.03	1141	1281	15.2	.31	.65	.87	961	912	34.8	.47	.81	.74	812	649	23.2	.14	.21	.95	.61	674	449	35.7
A356X	1.10	1433	.34	1.07	1168	1360	15.6	.26	.60	.93	1011	1020	41.3	.47	.81	.74	803	645	26.9	.12	.13	.93	.63	683	461	40.2
A370Y	1.10	1466	.30	1.09	1225	1424	18.7	.26	.56	.95	1072	1091	47.1	.54	.84	.70	786	587	21.8	.11	-	.95	.61	683	443	41.2
A358X	1.10	1472	.32	1.07	1177	1392	17.4	.25	.57	.93	1022	1049	41.5	.49	.81	.71	779	613	22.6	.13	.27	.94	.59	651	426	35.6
A355X	1.11	1489	.31	1.09	1193	1413	23.3	.29	.60	.93	1017	1033	38.7	.51	.82	.73	801	640	22.6	.13	.21	.95	.61	676	456	32.5
A369Y	1.18	1673	.29	1.17	1300	1638	18.0	.24	.53	.99	1105	1171	59.5	.51	.80	.71	800	612	23.9	.12	-	.92	.60	678	442	42.5
A360X	1.20	1708	.32	1.16	1274	1620	17.3	.26	.58	.99	1087	1184	44.0	.50	.82	.75	814	664	26.0	.11	.24	.91	.65	714	512	39.0
A366Y	1.22	1789	.30	1.20	1313	1724	23.3	.24	.54	1.02	1115	1246	52.1	.51	.81	.73	801	643	23.6	.12	.14	.93	.60	664	443	41.7
R-11X	1.62	2445	.29	1.60	1686	2348	12.5	.22	.51	1.37	1443	1721	62.0	.52	.81	.93	987	804	33.0	.14	.14	.95	.75	865	618	42.5
R-12Y	1.62	2455	.27	1.57	1683	2319	15.0	.18	.45	1.44	1539	1940	66.0	.54	.81	.88	946	729	33.0	.16	.33	.97	.69	741	449	40.5
R-9X	1.63	2502	.26	1.58	1717	2383	17.0	.22	.48	1.41	1521	1868	61.0	.50	.76	1.04	1128	1025	34.0	.13	.39	.81	.98	1062	908	36.0
R-7X	1.66	2709	.28	1.60	1772	2495	21.0	.17	.45	1.41	1571	1961	56.0	.51	.79	.92	1020	827	34.0	.14	-	.93	.77	882	574	36.5
R27-2Y	1.67	2718	.29	1.64	1817	2597	27.0	.18	.47	1.39	1538	1859	77.0	.49	.78	.95	1056	874	33.0	.17	.22	.95	.76	846	561	43.0
R-10X	1.70	2723	.28	1.69	1789	2649	14.0	.20	.48	1.49	1576	2057	67.5	.50	.78	1.04	1106	1010	37.0	.10	.15	.88	.91	964	767	49.0
R-6X[c]	1.67	2660	.27	1.62	1760	2485	24.5	.15	.42	1.51	1639	2151	45.0	.50	.77	1.15	1244	1238	27.0	.34	.30	1.11	.76	824	542	41.5
R-4X[c]	1.68	2660	.27	1.63	1747	2503	19.0	.14	.41	1.53	1631	2179	43.0	.54	.81	1.14	1221	1216	26.0	.33	.37	1.14	.83	881	631	37.0
R-5X[c]	1.67	2695	.26	1.61	1726	2486	19.0	.25	.51	1.43	1534	1958	46.6	.50	.76	1.18	1268	1336	27.0	.36	.47	1.12	.81	871	627	37.0

[a] W = 2005 lb for aircraft (A) drops and W = 2140 lb for rocket-boosted (R) tests; X and Y refer to parachute manufacturer.

[b] RMS = 0.506 sec with standard deviation of 0.020 sec.

[c] = 15.5 ft (L_R = 19.25 ft for all other tests)

(17.6 m²). These steady-state drag areas were determined as illustrated in Fig. 10. The calculated effective diameter of the reefed parachute is 14.3 ft (4.36 m). Optical data indicate that the inflated diameter of the aft portion of a reefed ribbon parachute is considerably larger than the reefing line circle diameter; hence, it was reasoned that an effective diameter based on drag area would be more representative for filling time calculations. The calculated values of filling time shown in Fig. 7 are approximately 20% lower than the data but the trend with velocity appears approximately correct.

Greene[8] recently correlated parachute inflation times (based on an opening distance concept) for deployment Mach numbers up to three. His correlation for opening distance is

$$L = (\rho_c/\rho_\infty)\alpha D_0 \tag{3}$$

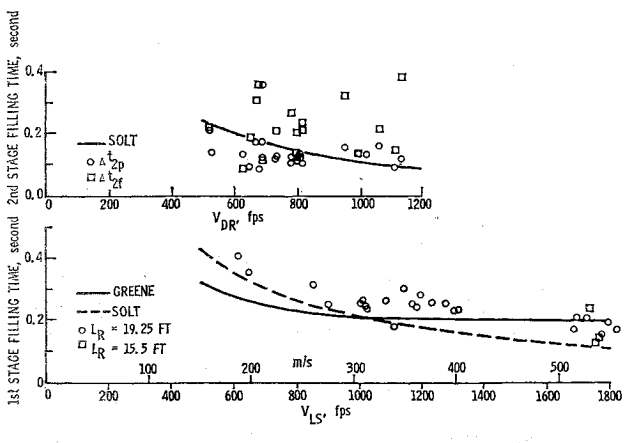

Fig. 7 Comparison of predicted and measured canopy filling times.

where $\alpha = V_c/(A_i - A_e)D_0$. Greene used values of α of 8 and 10 to correlate the data for 12.5 to 15% geometric porosity disk-gap-band or modified ring-sail parachutes. The higher value of α represents a higher porosity, hence, $\alpha = 10$ was used in the present calculation along with the effective diameter, D_E, in place of D_0. The filling times were then calculated from

$$\Delta t_{1p} = 10\,\rho_c D_E/\rho_\infty V_{LS} \tag{4}$$

The calculated reefed stage filling times, using Greene's method, are in fair agreement with the measured values in Fig. 7.

An attempt was made to adapt Eq. (1) to calculate the filling time of the second stage, Δt_{2f}, of the parachute. It was reasoned that the filling time of a nonreefed parachute minus the filling time of the same parachute to the reefed condition should represent the second stage filling time (i.e., from disreefing to full open). Hence

$$\Delta t_{2f} = \Delta t_f - \Delta t_{1p} \tag{5}$$

where

$$\Delta t_f = 0.65\lambda_G D_c/V_{DR} \tag{6}$$

$$\Delta t_{1p} = 0.65\lambda_G D_E/V_{DR} \tag{7}$$

The calculated values agree fairly well with the measured time to second peak load, Δt_{2p}, in Fig. 7; however, in general, the filling time from the optical data is greater.

The snatch load and the first stage opening shock loads are presented vs line stretch dynamic pressure in Fig. 8. Each data point represents the average peak load of the accelerometer channels (usually three) for each test. The data are fairly consistent and repeatable. Some of the scatter is probably due to slightly different parachute construction

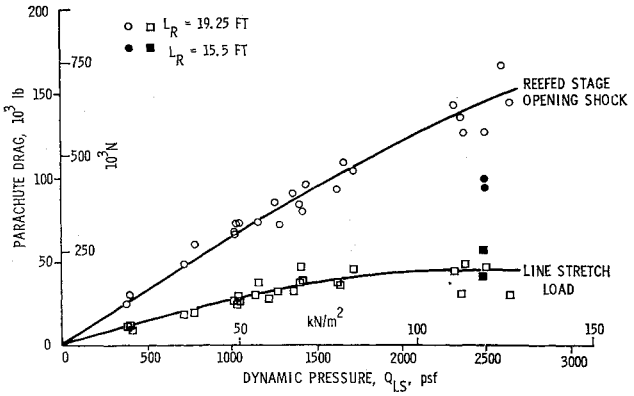

Fig. 8 Snatch and reefed-stage opening shock loads.

techniques and packing methods. The parachute manufacturer is noted in Table 1. Examination of the 35-mm ground documentary film indicated rather severe pitching of the test vehicle during parachute deployment at transonic speeds (the tail can was ejected 0.6 sec after test vehicle release from the aircraft). This vehicle angle of attack and pitching velocity resulted in nonsymmetric stripping of the bag from the canopy and asymmetric filling of the first stage, which would explain some of the data scatter in Fig. 8. The snatch load appears to become asymptotic at the higher dynamic pressure. The 200-lb (890-N) break lines (for tying the canopy and shroud lines to the deployment bag) appear to be effective in providing orderly deployment which reduces the snatch load. Note that the snatch load is only approximately one-third the peak opening shock load at the highest dynamic pressure. The peak opening shock load is not a linear function of dynamic pressure at line stretch. The peak opening shock of the parachute with the 15.5-ft (4.7-m) reefing line is only about two-thirds the load measured with the 19.25-ft (5.87-m) reefing line. These same averaged parachute peak opening load drag data are plotted vs dynamic pressure at first peak load in Fig. 9. These loads are compared with loads calculated from the averaged steady state reefed drag area values determined in Fig. 10.

Averaged drag areas for the two reefed stage configurations and the full open ribbon parachute are presented as a function of Mach number at first or second peak load in Fig. 10. The reefed drag area values were determined by taking an arithmetic average of drag areas calculated every 0.05 sec from the first peak load to disreefing time. Average drag areas are 78 ft^2 (7.25 m^2) and 46 ft^2 (4.27 m^2) for the 19.25-ft (5.87-m) and 15.5-ft (4.7-m) reefing line lengths, respectively. It is considered significant that the reefed drag area is essentially constant from $0.5 \leq M_{1p} \leq 1.5$. The drag coefficient of the

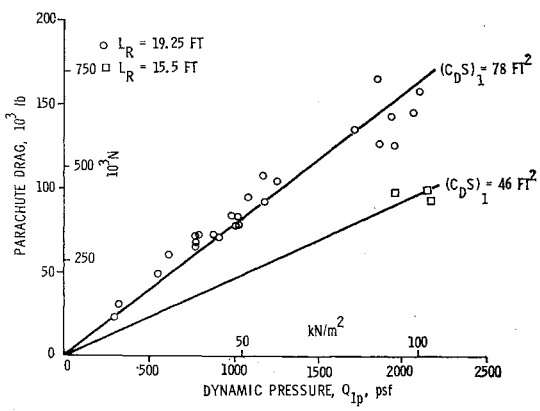

Fig. 9 Comparison of reefed stage opening shock loads with steady-state values.

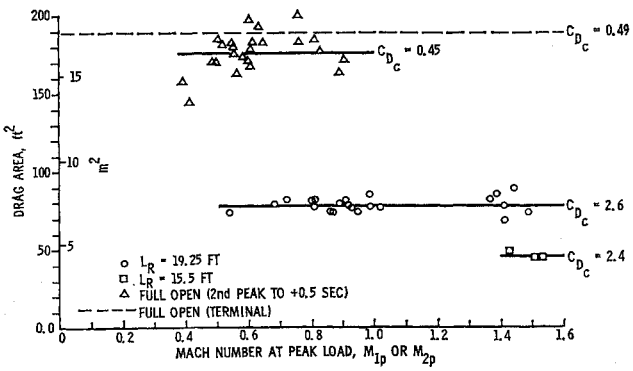

Fig. 10 Steady-state drag areas for reefed and full open parachute.

reefed parachutes ($C_{D_c} \approx 2.5$) is based on area of the reefing line circle. These drag coefficient data are about a factor of three higher than drag coefficients determined from a $M = 1.8$ wind-tunnel test of a 1.73-ft (0.53-m) diam ribbon parachute (Solt,[4] p. 188). Steady-state drag areas for the second stage (full open) were obtained by averaging drag areas calculated every 0.05 sec for 0.5 sec after the second peak load. These drag area data evidence considerable scatter from test to test—an average $(C_DS)_2$ value of 176 ft^2 (16.35 m^2) yields a drag coefficient, $C_{D_c} = 0.45$. An average terminal drag area value of 189 ft^2 (17.6 m^2) [standard deviation of 11 ft^2 (1 m^2)] was determined by computer trajectory calculations by matching the experimentally-determined (from theodolites) trajectories for 11 tests. The drag coefficients, $C_{D_c} = 0.45$ and 0.49, agree well with data presented by Solt.[4]

The ratio of drag areas at peak loading to the steady-state drag area (given in Fig. 10) are presented vs Mach number in Fig. 11. The curves drawn result from a computer program which fit a second degree polynomial to the data by the least squares method. The data for a reefing line length of 15.5 ft (4.72 m) were not included in the curve fitting calculations. The bottom plot shows the ratio with the reefed drag area at peak load calculated based on the dynamic pressure at line stretch. This definition of amplification factor may be of more value to the design engineer as he can accurately estimate a priori the dynamic pressure at line stretch. This first stage drag area ratio for $L_R = 19.25$ ft (5.87 m) is approximately 0.9 subsonically and 0.7 supersonically, whereas the drag area ratio for $L_R = 15.5$ ft (4.7 m) is approximately 0.8 supersonically. The higher amplification factor for the shorter reefing line is due to smaller vehicle deceleration during canopy opening.

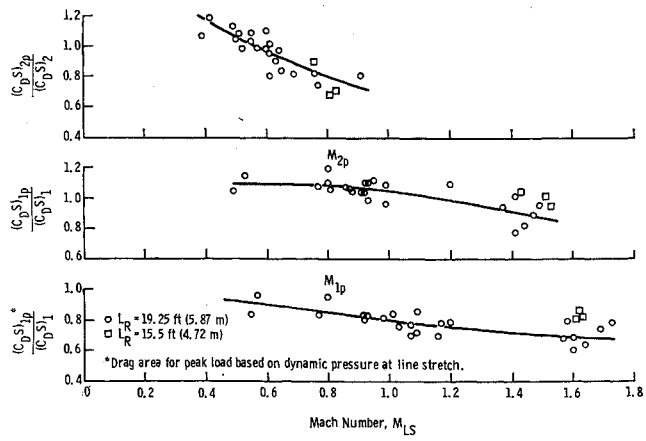

Fig. 11 Effect of Mach number on the drag area at peak opening shock conditions.

The amplification or "X" factor for the reefed chute is presented in the middle plot as a function of Mach number at peak load. The "X" factor is approximately 1.1 subsonically and 0.9 supersonically. Even with the considerable data scatter there appears to be a Mach number effect on the "X" factor. The "X" factor (see Solt[4]) is normally defined as the ratio between the maximum opening force and the constant drag force. Solt indicates a typical value for a ribbon parachute, under near-infinite mass conditions, is $X \geq 1.1$ with some decrease for transonic and supersonic deployment. The decrease in "X" factor with Mach number may be due to the fact that, because of the high deceleration (i.e., 35 to 77 g's transonically and supersonically), the peak parachute loading occurs before the reefed canopy is fully inflated.

Finally, the amplification or "X" factor for the disreefed canopy is shown in the top plot in Fig. 11 as a function of Mach number at peak load. The data show a consistent decrease of "X" from about 1.1 to 0.7 as M_{2p} increases from 0.4 to 0.9. This decrease in the effective "X" factor with Mach number is due to the high deceleration (15–50 g's) and occurrence of the peak parachute load before the canopy is fully inflated. Comparison of filling time to peak load, Δt_{2p}, with filling time, Δt_{2f}, to full open from Table 1 and Fig. 7 illustrates this point even though the Δt_{2f} times are not very consistent.

Flight data for heavy duty ribbon parachutes illustrating the effect of reefing line length on drag area for 16-ft to 76-ft (4.88-m to 23.16-m) diam parachutes tested by Sandia Laboratories is given by Pepper[2] and Pepper and Maydew.[1] These data are for high subsonic, transonic, and low supersonic deployment of the reefed canopies. The reefed drag area data for the 22.2-ft (6.8-m) diam parachute agree well with the previous data for the 16-, 20-, and 24-ft (4.88-, 6.1-, and 7.3-m) diam parachutes.

Conclusions

Analysis of the data from the 29 flight tests indicates the following. 1) The maximum measured snatch load, reefed stage opening shock, and second stage opening shock are 65 klb (289 kN), 165 klb (734 kN), and 150 klb (667 kN), respectively. 2) The measured load data and parachute function times are consistent and repeatable. 3) The time from tail-can-ejection to reefed stage inflation decreased from about 1 to 0.5 sec as the test Mach number increased from 0.57 to 1.70. 4) The measured filling times of the reefed (first) stage agrees fairly well with predicted values. 5) There is no measurable effect of Mach number on the steady-state drag area of the reefed canopy at Mach numbers from 0.50 to 1.50. 6) The drag coefficients of 0.45 to 0.49 for the fully open canopy agree well with previous data. 7) The ratio of reefed stage peak load drag area to steady state drag area (an amplification or "X" factor) decreases from about 1.1 subsonically to about 0.9 supersonically. 8) The second stage "X" factor decreases from about 1.1 to 0.7 as the Mach number increases from 0.4 to 0.9.

References

[1] Pepper, W. B., Jr. and Maydew, R. C., "Aerodynamic Decelerators—An Engineering Review," *Journal of Aircraft*, Vol. 8, No. 1, Jan. 1971, pp. 3–19.

[2] Pepper, W. B., Jr., "Parachute Design and Performance for Supersonic Deployment and for the Recovery of Heavy Loads," presented at Deutsche Gesellschaft fur Luft-und Raumfahrt E. V., Deutsche Forschungs-und Versuchsanstalt, and Advisory Group for Aerodynamic Deceleration, Technical University of Braunschweig, West Germany, Sept. 15–19, 1969; also SC-DC-69-1883, 1969, Sandia Labs., Albuquerque, N. Mex.

[3] Pepper, W. B., Jr., "Recent Flight-Test Results in Deploying a 20-ft Diameter Ribbon Parachute," *Journal of Aircraft*, Vol. 6, No. 1, Jan.-Feb. 1969, pp. 74–76; also "A 20-ft Diameter Ribbon Parachute for Deployment at Dynamic Pressures Above 4000 PSF," *Journal of Aircraft*, Vol. 4, No. 3, May-June 1967, pp. 266–267.

[4] Solt, G. A., Jr., "Performance of and Design Criteria for Deployable Aerodynamic Decelerators," ASD-TR-61-579, Dec. 1963, Air Force Flight Dynamics Lab., Wright-Patterson Air Force Base, Ohio.

[5] Gallagher, J. P., "Reefing Line Cutter," U.S. Patent 3,335,493, Aug. 15, 1967, Sandia Labs., Albuquerque, N. Mex.

[6] Widdows, H. E., "Parachute Deployment Control Assembly," U.S. Patent 3,145,956, Aug. 25, 1964, Sandia Labs., Albuquerque, N. Mex.

[7] Summary, SMSTFACS-O, April 1967, Sandia Labs. Field Test Facilities, Albuquerque, N. Mex.

[8] Greene, G. C., "Opening Distance of a Parachute," *Journal of Spacecraft and Rockets*, Vol. 7, No. 1, Jan. 1970, pp. 98–100.